Available online at www.sciencedirect.com
ScienceDirect
ELSEVIER
Journal of Luminescence 121 (2006) 349–352
JOURNAL OF LUMINESCENCE
www.elsevier.com/locate/jlumin

Photoluminescence properties of SiN_x/Si amorphous multilayer structures grown by plasma-enhanced chemical vapor deposition

B.M. Monroy[a], G. Santana[a,*], J. Aguilar-Hernández[b], A. Benami[a], J. Fandiño[c], A. Ponce[c], G. Contreras-Puente[b], A. Ortiz[a], J.C. Alonso[a]

[a]Instituto de Investigaciones en Materiales, Universidad Nacional Autónoma de México, Ciudad Universitaria, A.P. 70-360, Coyoacán 04510, D.F., México
[b]Escuela Superior de Física y Matemáticas del Instituto Politécnico Nacional, Edificio 9, U.P.A.L.M., 07738 D.F., México
[c]Instituto de Física, Universidad Nacional Autónoma de México, Cd. Universitaria, A.P. 20 364, Coyoacán 04510, D.F., México

Available online 12 September 2006

Abstract

Very thin (nanometric) silicon layers were grown in between silicon nitride barriers by $SiH_2Cl_2/H_2/NH_3$ plasma-enhanced chemical vapor deposition (PECVD). The multilayer structures were deposited onto fused silica and silicon substrates. Deposition conditions were selected to favor Si cluster formation of different sizes in between the barriers of silicon nitride. The samples were thermally treated in an inert atmosphere for 1 h at 500 °C for dehydrogenation. Room-temperature photoluminescence (RT-PL) and optical transmission in different ranges were used to evaluate the optical properties of the structures. UV–VIS absorption spectra present two band edges. These band edges are well fitted by the Tauc model typically used for amorphous materials. RT-PL spectra are characterized by strong broad bands, which have a blue shift as a function of the deposition time of the silicon layer, even for as-grown samples. The broad luminescence could be associated with the confinement effect in the silicon clusters. After annealing of the samples, the PL bands red shift. This is probably due to the thermal decomposition of N–H bonds with further effusion of hydrogen and better nitrogen passivation of the nc-Si/SiN_x interfaces.
© 2006 Elsevier B.V. All rights reserved.

PACS: 73.61.Tm; 78.40.Fy; 78.55.−m

Keywords: Silicon nanoclusters; PECVD; Silicon nitride; Multilayer; Photoluminescence

1. Introduction

Silicon nanoclusters (nc-Si) in silicon oxide (SiO_2) or silicon nitride (Si_3N_4) matrices constitute a very attractive alternative of opto-electronic materials compatible with the actual Si technology [1]. Previous studies have demonstrated photoluminescence (PL) from crystalline or amorphous nc-Si sandwiched between layers of larger gap materials such as SiO_2 or SiN_x [2–6]. The particular interest in the nc-Si/SiO_2 and nc-Si/SiN_x multilayer structures or superlattices is due to the high control over the nc-Si layer thickness that can be achieved, which is one of the key requirements for controlling their photoluminecent properties and device applications [2]. The emission wavelengths reported for these superlattices after being subjected to annealing processes are mainly located in the near infrared (IR) and visible (650–800 nm) regions. Among the different mechanisms proposed for explaining the radiative recombination processes, the most accepted one is related to quantum confinement effects (QCE), in which the emission features depend strongly on the size of the nc-Si layers [5,6]. However, many features of the optical emission and properties of these materials, as well as the role of surface and/or interfaces between nc-Si and matrix are still controversial and need to be clarified.

In the present work, very thin layers of nc-Si were grown in between SiN_x layers using $SiH_2Cl_2/H_2/NH_3$ plasma-enhanced chemical vapor deposition (PECVD). The PL characteristics of as-grown and annealed samples are investigated and the possible PL mechanisms are discussed.

*Corresponding author. Tel.: +52 55 56 22 46 06;
fax: +52 55 56 16 12 51.
E-mail address: gsantana@zinalco.iimatercu.unam.mx (G. Santana).

0022-2313/$ - see front matter © 2006 Elsevier B.V. All rights reserved.
doi:10.1016/j.jlumin.2006.08.046

The use of SiH_2Cl_2 as silicon precursor was motivated by previous works which have demonstrated that the use of chlorinated silanes as precursor gases favors the as-grown crystallinity of the nc-Si, which has a direct influence on the PL emission due to QCE [7].

2. Experimental details

Thirty-six period superlattices of nc-Si/SiN_x were deposited by PECVD using a conventional radio-frequency (13.56 MHz), parallel-plate (150 cm^2 in area, 1.5 cm apart) system. The films were deposited on fused silica and (1 0 0) n-silicon high-resistivity substrates for their optical and structural characterization, respectively. Substrates were subjected to a standard cleaning procedure (which includes etching in diluted hydrofluoric acid in the case of silicon) immediately before loading them into the deposition chamber.

The nc-Si layers were grown using an $SiH_2Cl_2/H_2/Ar$ mixture at a chamber pressure of 500 mTorr and plasma power of 10 W. The SiH_2Cl_2 and H_2 flow rates were 2 and 100 sccm, respectively. The thickness of the nc-Si layers was controlled by deposition time (20 and 30 s). Si_3N_4 barriers were deposited using an $SiH_2Cl_2/NH_3/Ar$ mixture with $[NH_3]/[SiH_2Cl_2]$ flow ratio of 2.5 at 350 mTorr and 30 W. The details on the structural and dielectric properties of these SiN_x films are reported elsewhere [8]. The deposition time for all the SiN_x layers was 2 min, except for the first and last layers of the whole superlattice, which was of 5 min. The Ar flow rate was 50 sccm for both nc-Si and SiN_x processes. In all cases the substrate temperature was kept at 200 °C. After deposition, samples were dehydrogenized in nitrogen (N_2) atmosphere for 1 h at 500 °C.

For the structural characterization, the high-resolution transmission electron microscopy (HRTEM) technique was used in a cross-section sample. Mechanical grinding procedures and ion milling processes have been employed for the electron-transparency thinning of the specimen. The HRTEM studies were carried out in a field emission gun microscope (JEM-2010 F), which operates at 200 kV and the images have been obtained near the Scherzer focus. The HRTEM images have been recorded with an on-line CCD camera and treated with a digital analysis program. The refractive index and thickness of the films were measured with a Gaertner L117 Ellipsometer equipped with an He–Ne laser ($\lambda = 632.8$ nm). The bonding structure of the films was analyzed by means of a Fourier Transform InfraRed (FTIR) spectrometer (Nicolet-210). PL studies were carried out at room temperature in a conventional PL system described in detail elsewhere [9]. An He–Cd laser ($\lambda = 325$ nm) at 10 mW was employed as the excitation source. The outgoing radiation from the sample was focused on the entrance slit of a 1403-SPEX double monochromator. The detection was carried out using a RCA-C31034 photomultiplier thermoelectrically cooled coupled to a photon counter. All the spectra were corrected for the spectral response of the system.

3. Results and discussion

The samples consist of 37 amorphous SiN_x barriers with 36 nc-Si layers or fractional layers in between. As the cross-section HRTEM image of Fig. 1 shows, the thickness of the SiN_x layers is around 28 nm; meanwhile that of the nc-Si layers deposited during 20 s is of approximately 2 nm. The inset of Fig. 1 shows that the height of the Si nanoclusters is constrained by the SiN_x barriers, but their lateral sizes are more than one order of magnitude larger. The measured refractive index of both samples was 1.75, which corresponds to the SiN_x matrix. The superlattice complete thickness was around 1000 nm in both samples.

FTIR transmission spectra for the as-grown and annealed samples are shown in Figs. 2(a) and (b), respectively. In addition to the prominent band centered at 900 cm^{-1}, two other peaks are discernible at 1170 and 3330 cm^{-1}. These features are characteristic of the SiN_x matrix and can be assigned to the Si–N stretching, N–H bending and N–H stretching vibration modes, respectively. The peak localized between 480 and 500 cm^{-1} is assigned to the Si–Si vibration mode characteristic of the silicon film grown in between the Si_3N_4 barriers. It is worth noting that there is no feature around 2100–2230 cm^{-1}, which indicates the absence of Si–H bonds in these multilayer structures.

Room-temperature (RT) PL spectra of the as-grown samples are shown in Fig. 3. PL spectra consist mainly of two intense bands associated to quantum confinement in the nc-Si. In the case of the 30 s sample, the two principal peaks are centered around 680 and 600 nm. A blue shift is clearly observed for the 20 s sample where the principal

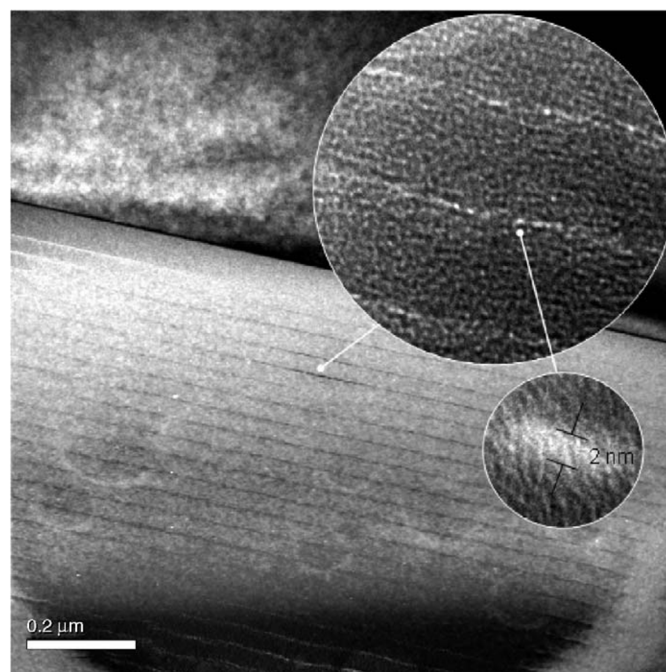

Fig. 1. HRTEM micrograph showing the multilayer structure of the 20 s sample. The insets show a magnification of the SiN_x barriers and the silicon cluster.

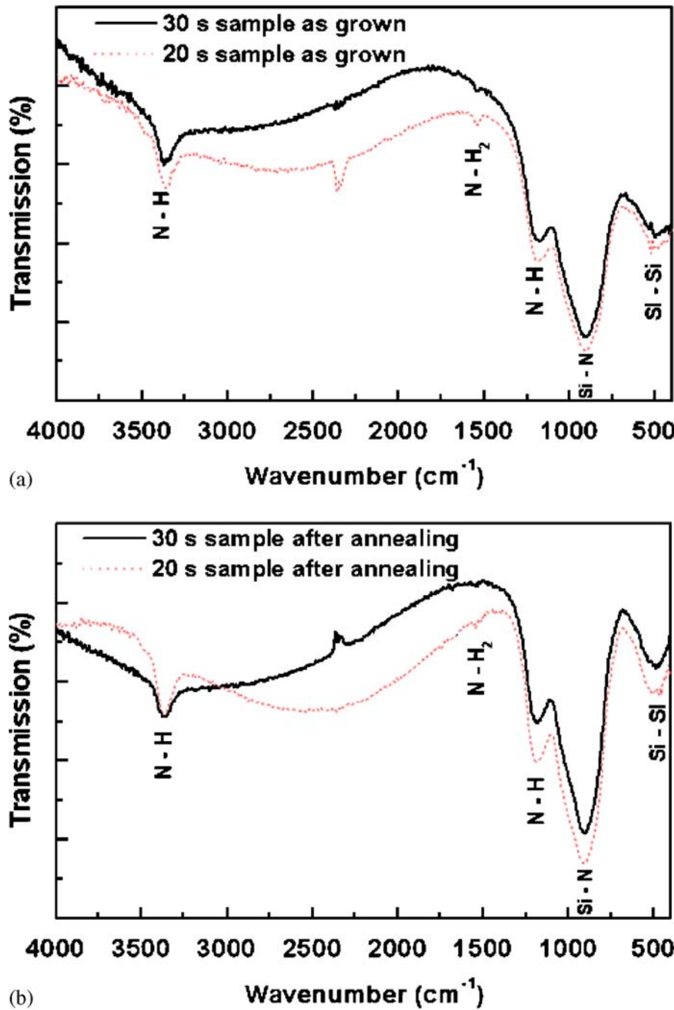

Fig. 2. FTIR transmission spectra of (a) as-grown samples and (b) samples after annealing.

peaks are at 630 and 560 nm. As Fig. 1 shows, the confinement of the nc-Si in this type of structures occurs mainly in the direction perpendicular to the surface of the layers. According to this and since the use of dichlorosilane favors low hydrogen content and crystallinity of the nc-Si [7,10], the 1D (one-dimensional)-QCE model given by the equation $E_{\text{peak}} = 1.16 + 3.9/d^2$ can be used to correlate the main PL peaks (E_{peak}) with the nc-Si layer thicknesses (d) [12,13]. Thus, the two main peaks of the PL spectra for the as-grown samples (Fig. 3) indicate that the average nc-Si layer thicknesses are in the range of 2.4–2.1 and 2.2–1.9 nm for the 30 and 20 s samples, respectively. It is worth noting that the value of d for the 20 s sample is in very good agreement with the corresponding thickness observed by HRTEM. On the other hand, under this QCE model, the blue shift in the PL of the 20 s sample with respect to that of the 30 s is directly explained as a result of the reduction of the nc-Si average thickness. The weaker peaks centered around 450 nm observed in both spectra of Fig. 3, which seem to be independent of nc-Si size, can be associated to recombination via interface levels [3,4].

The PL emission of the annealed samples can be observed in Fig. 4. There is no significant change of PL intensity after dehydrogenation of the samples, although there are some changes in the structure of the spectra and a small red shift. At present, the origin of these changes is not clear, but they could be associated with changes in the passivation state of the nc-Si/SiN$_x$ interfaces, similar to those occurring in three-dimensional confined nc–Si, produced by the thermal decomposition of N–H bonds with further effusion of hydrogen [10,11,14]. The insets in Fig. 4 show the PL spots with the corresponding emission colors, as can be seen with the naked eye in the darkened room.

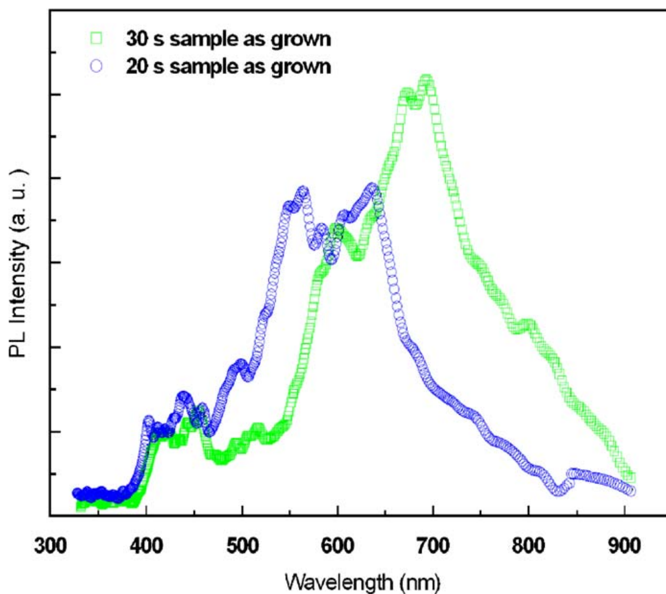

Fig. 3. PL emission spectra of as-grown samples with different deposition times.

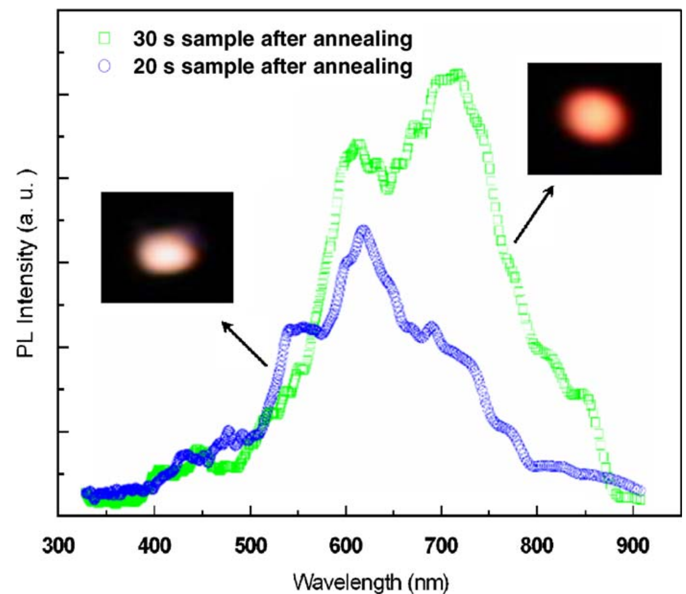

Fig. 4. PL emission spectra of samples after dehydrogenation process. The insets show the PL spot as seen with the naked eye in a dark room.

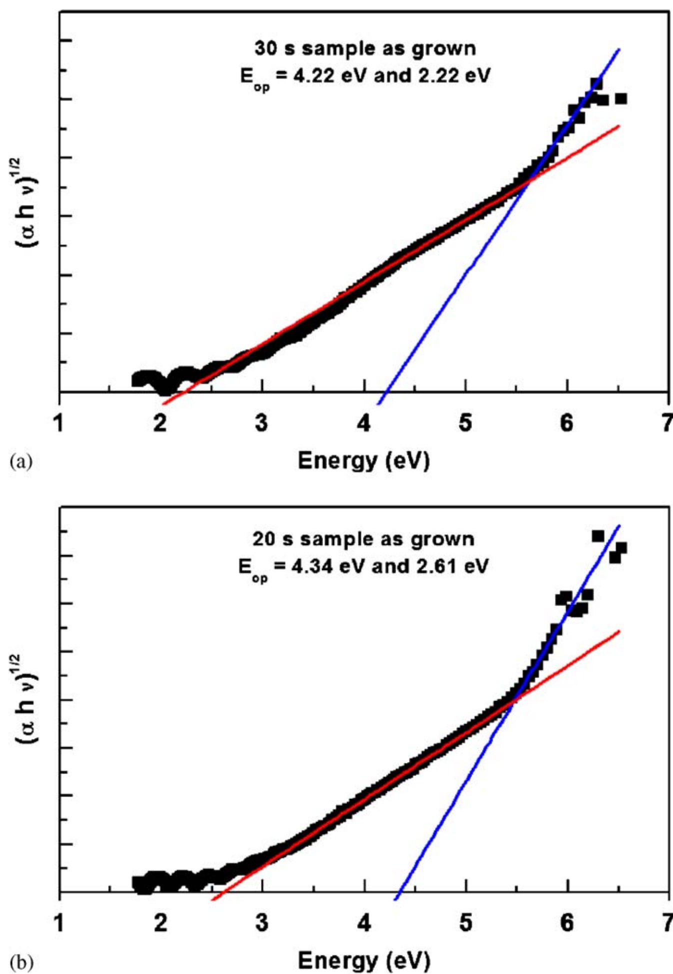

Fig. 5. Tauc plots of samples with deposition times of (a) 30 s and (b) 20 s.

Tauc plots of absorbance spectra for samples grown onto fused silica substrates are displayed in Fig. 5. Two distinct absorption edges can be observed corresponding to the Si_3N_4 matrix band gap (~4.2 eV) and the nc-Si band gap. There is a red shift from 2.6 eV (20 s) to 2.2 eV (30 s) in the nc–Si band gaps as a function of the deposition time. The difference between the observed optical and band gaps is due to the Stokes shift (Franck–Condon effect) [13].

4. Conclusions

The use of chlorinated silanes in SiN_x/nc-Si/ SiN_x multilayers deposited by PECVD allows easier control of the silicon clusters size and crystallinity. This has a direct effect on the intense PL emission, which was observed in the visible region from as-grown samples. The principal PL emission can be tuned by the deposition time of the nc-Si layer and is attributed to QCE.

Acknowledgments

We acknowledge the technical assistance of L. Huerta, M.A. Canseco, C. Flores, J. Santoyo, J. Camacho, S. Jimenez, the technical support of Departamento de Ciencias e Ingeniería de los Materiales e I. M. y Q. I., Facultad de Ciencias-Universidad de Cadiz and partial financial support for this work from CONACyT-México, under project 47303-F, PAPIIT-UNAM under projects IN-109803 and IN-114406-2.

References

[1] L. Pavesi, J. Phys.: Condens. Matter 15 (2003) R1169.
[2] D.J. Lockwood, L. Tsybeskov, Encyclopedia Nanosci. Nanotechnol. 6 (2004) 477.
[3] K. Chen, Z. Ma, X. Huang, J. Xu, W. Li, Y. Sui, J. Mei, D. Zhu, J. Non-Cryst. Solids 338–340 (2004) 448.
[4] H.B. Kim, J.H. Son, C.N. Wang, K.H. Chae, Thin Solid Films 467 (2004) 176.
[5] L. Wang, Z. Ma, X. Huang, Z. Li, J. Li, Y. Bao, J. Xu, W. Li, K. Chen, Solid State Commun. 117 (2001) 239.
[6] S. Nihonyanagi, K. Nishimoto, Y. Kanemitsu, J. Non-Cryst. Solids 299–302 (2002) 1095.
[7] H. Shirai, Y. Fujimura, S. Jung, Thin Solid Films 407 (2002) 12.
[8] G. Santana, J. Fandiño, A. Ortiz, J.C. Alonso, J. Non-Cryst. Solids 351 (2005) 922.
[9] J. Aguilar-Hernández, G. Contreras-Puente, J.M. Figueroa-Estrada, O. Zelaya-Angel, Jpn. J. Appl. Phys. 33 (1994) 37.
[10] G. Santana, B.M. Monroy, A. Ortiz, L. Huerta, J.C. Alonso, J. Fandiño, J. Aguilar-Hernández, E. Hoyos, F. Cruz-Gandarilla, G. Contreras-Puentes, Appl. Phys. Lett. 88 (2006) 1916.
[11] A.D. Yoffe, Adv. Phys. 42 (1993) 173.
[12] T.Y. Kim, N.M. Park, K.H. Kim, G.Y. Sung, Y.W. Ok, T.Y. Seong, C.J. Choi, Appl. Phys. Lett. 85 (2004) 5355.
[13] C. Delerue, G. Allan, M. Lannoo, Semicond. Semimet. 49 (1998) 253.
[14] A. Puzder, A.J. Williamson, J.C. Grossman, G. Galli, J. Chem. Phys. 117 (2002) 6721.